

This is an authors' final version of the manuscript of "Double the dates and go for Bayes | impacts of model choice, dating density and quality on chronologies" by Maarten Blaauw (Queen's University Belfast), Andrés Christen (CIMAT, Guanajuato), Keith Bennett (St Andrews) and Paula Reimer (Queen's University Belfast). It contains errors that were corrected at proof stage, so should not be used. It is provided here solely in compliance with the requirements of HEFCE for REF: see <http://www.hefce.ac.uk/pubs/year/2014/201407/>.

The publisher's final version is available at <https://doi.org/10.1016/j.quascirev.2018.03.032>, or by contacting any of the authors.

1 Double the dates and go for Bayes — impacts of model
2 choice, dating density and quality on chronologies

3 Maarten Blaauw^{a,*}, J. Andrés Christen^b, K. D. Bennett^{c,d}, Paula J. Reimer^a

4 ^a*School of Natural and Built Environment, Queen's University Belfast, Belfast BT7 1NN,*
5 *Northern Ireland, United Kingdom*

6 ^b*Centro de Investigación en Matemáticas CIMAT, Guanajuato 36023, Guanajuato, Mexico*

7 ^c*School of Geography & Sustainable Development, University of St Andrews, St Andrews*
8 *KY16 9AL, Scotland, United Kingdom*

9 ^d*Queen's Marine Laboratory, Queen's University Belfast, Portaferry BT22 1PF, Northern*
10 *Ireland, United Kingdom*

11 **Abstract**

12 Reliable chronologies are essential for most Quaternary/geological studies, but
13 little is known about how age-depth model choice as well as dating density and
14 quality affect the precision and accuracy of chronologies. A meta-analysis
15 suggests that most existing late-Quaternary studies contain fewer than one
16 date per millennium, and thus provide millennial-scale precision at best. We
17 use simulations to estimate what dating density and quality are required to
18 obtain accurate chronologies at a certain precision. For many studies, a
19 doubling in dating density would significantly improve chronologies and thus
20 their value for reconstructing and interpreting past environmental changes.
21 Commonly used basic age-depth models stop becoming more precise after a
22 certain dating density is reached, but Bayesian age-depth models, which take
23 advantage of chronological ordering, keep on improving with more dates.
24 Moreover, Bayesian models produce more realistic errors for cores with few
25 dates, and can reach multi-decadal precision at high resolution. Bayesian
26 age-depth models are also much more robust against dating scatter and
27 outliers. Our simulations show that basic age-depth models underestimate
28 uncertainty and are inaccurate at low dating densities, and perform poorly at
29 high dating densities. Bayesian age-depth models outperform basic ones at all
30 tested dating densities, qualities and time-scales. We recommend that

*Corresponding author: maarten.blaauw@qub.ac.uk
Preprint submitted to Elsevier

31 chronologies should be based on a minimum of 2 dpm wherever realistically
32 possible.

33 *Keywords:* age-depth model, radiocarbon dates, chronological uncertainties,
34 Bayesian statistics

35 INTRODUCTION

36 Whenever an additional level of a sedimentary site, core or event is dated, our
37 knowledge of its chronology increases (Bennett, 1994; Bennett and Fuller,
38 2002). However, dating is expensive and time-consuming, and it can prove
39 challenging to collect sufficient reliable material for dating. A single
40 radiocarbon (^{14}C) date often costs several hundred dollars, and waiting times
41 can amount to months, or even years if several iterations of dating are
42 required. Moreover, radiocarbon and other scientific dates have laboratory
43 errors, the size of which reflects measurement uncertainties as well as the
44 nature of laboratory sample treatment. Sites extending further back in time
45 generally have larger absolute dating errors and thus lower precision age-depth
46 models. Typical relative ^{14}C dating errors hover around 1% (0.5% for modern
47 AMS systems), however lower sample sizes can result in larger errors although
48 higher-precision dates can be obtained with longer counting times. Given the
49 many ways through which ^{14}C or other absolute dates can be offset from their
50 actual age, some degree of scatter is unavoidable in sequences of dates.

51 Repeated measurements of single samples within and between laboratories
52 sometimes show more scatter than can be accounted for by reported errors
53 (Bronk Ramsey et al., 2004; Christen and Pérez E., 2009; Scott, 2013),
54 perhaps owing to inhomogeneous sampling or laboratory-introduced offsets.
55 At times high-resolution ^{14}C dating can reveal unexpectedly large scatter for
56 some core sections (e.g. Lohne et al., 2013; Groot et al., 2014).

57 Data in the Neotoma Palaeoecology Database (neotomadb.org) show that
58 since the 1960s the majority of late Quaternary sites have been dated using
59 just a few ^{14}C dates (median 5 dates per core), equivalent to ca 1 date every

60 1400 years or 0.72 dates per millennium (dpm) (Figure 1). Only a very few
61 sites reach much higher dating densities of ca 10–30 dpm (e.g. Kilian et al.,
62 1995; Gulliksen et al., 1998; Lohne et al., 2013; Mauquoy et al., 2002; Blaauw
63 et al., 2004; Southon et al., 2012). For the last 15 years, mean dating density
64 is slightly higher, at 1.3 dpm. Only 14% of the sites have > 2 dpm; 2% have
65 > 4 dpm.

66 Here we investigate: (i) whether current typical dating densities are sufficient;
67 (ii) the degree to which higher dating densities enhance chronologies; (iii)
68 whether certain types of age-depth models provide more realistic estimates of
69 precision and accuracy (Telford et al., 2004; Parnell et al., 2011; Trachsel and
70 Telford, 2017); and (iv) the extent to which chronologies are affected by dating
71 error, scatter and outliers. Our analysis of existing cores enables estimates of
72 chronological precision, but not accuracy because the ‘true’ sedimentation
73 histories of the sites are unknown. Therefore we also use a three-staged
74 simulation approach of (i) modelling the accumulation over time of a site
75 (sim_{acc}); (ii) producing a range of basic and Bayesian age-depth models
76 (sim_{age}) and comparing them to the true sim_{acc} timeline; and (iii)
77 sequentially adding single dates (sim_{dat}) using a sampling strategy after
78 Christen and Sansó (2011), followed by re-running the age-depth models
79 (sim_{age}), repeating as necessary. To test the chronological impact of dating
80 quality, we simulated a range of values for dating error and scatter, as well as
81 outlying dates. Most simulated cores spanned several metres, but some were
82 shorter, high-resolution sections.

83 METHODS

84 We used a three-step process on cores with both low and high dating density
85 cores for our analysis. First the accumulation rate (sim_{acc}) was simulated to
86 obtain an estimated calendar date for each core (θ_d). Then we assigned a
87 radiocarbon date based on the IntCal13 calibration curve with random
88 variation within in assigned limits. Finally we used a variety of age-depth

89 models and calculated the difference between the model age and our assigned
90 age to quantify which model worked better for the different data density cores.

91 *Data*

92 Age-depth models were applied to two datasets:

- 93 1. Cores from the entire Neotoma Palaeoecology Database
94 (neotomadb.org). We analysed the dating density of all cores with at
95 least two ^{14}C dates and spanning at least 500 yr.
- 96 2. The sequence at Kråkenes (western Norway, 61.48°N, 5.7°E: Gulliksen
97 et al., 1998; Lohne et al., 2013), which has 118 accelerator mass
98 spectrometry ^{14}C ages over the interval ca 14–8 kyr BP (so ca 20 dpm).
99 In order to estimate the effect of changing dating density, we removed all
100 but the topmost and bottommost dates, and then sequentially added
101 single dates (using the method outlined below) until reaching 20 dpm.

102 *Sedimentary sequences (sim_{acc})*

103 Besides real data sets, we also simulated hypothetical cores. Sedimentation
104 was simulated by modelling the deposition time represented within each depth
105 section $ds_i = d_i - d_{i-1}$ of a core (default every cm between 0 and 500 cm).

106 Unless stated otherwise, the deposition time at the topmost section was
107 sampled from a gamma distribution as in Blaauw and Christen (2011) with
108 $acc_1 \sim \text{Gamma}(acc.shape, acc.shape/acc.mean)$, defaults 50 yr cm^{-1} and 1.1
109 for mean and shape, respectively. Its top age, θ_0 , was set as 0 cal BP by
110 default. The deposition rate of each section ds_i was modelled to deviate from
111 the preceding section ds_{i-1} by a random value sampled from a uniform
112 distribution with width $2 acc.var$ (default 3.0), where deposition times could
113 not go below $acc.min$ (default 5.0 yr cm^{-1});

114 $acc_t \sim \max(acc.min, acc_{t-1} + \text{Unif}(-acc.var, acc.var))$. These simulated
115 deposition histories then provided the ‘true’ calendar age for each depth of the
116 simulated cores, θ_d .

117 We then simulated the initial and sequential (see later) dating of these
 118 artificial cores, sim_{dat} . For the simulations here, calibrated ^{14}C dates were
 119 modelled, but other types of dates could also be used. For each depth to be
 120 dated (see below), its ‘true’ calendar age θ_d was known from the simulated
 121 deposition history sim_{acc} . Uncertainty in having sampled contemporaneous
 122 material was then simulated by adding random variation x_{scat} (default 10 yr)
 123 from a normal distribution $\theta' \sim N(\theta, x_{scat}^2)$. Additionally, with a probability
 124 p_{out} (default 5%), the calendar date was treated as an outlier and shifted by
 125 up to x_{shift} (default 1000) years:

$$\theta'' = \begin{cases} \text{Unif}(\theta' - x_{shift}, \theta' + x_{shift}) & p_{out} \\ \theta' & 1 - p_{out} \end{cases} \quad (1)$$

126 Then we used the IntCal13 ^{14}C calibration curve (Reimer et al., 2013), which
 127 provides estimates of the ^{14}C age μ_θ for each calendar age θ . We simulated a
 128 ^{14}C date with some scatter by taking the IntCal13 ^{14}C age of θ'' , $\mu_{\theta''}$, and
 129 adding some scatter $y_{\theta''} \sim N(\mu_{\theta''}, \sigma^2)$ where the laboratory error
 130 $\sigma = \max(\sigma_{min}, y_{scat} \times \epsilon \times \mu_{\theta''})$, with σ_{min} the minimum error (default 20 ^{14}C
 131 yr), y_{scat} an error multiplier (default 1.5) and ϵ the analytical uncertainty
 132 (default 1%)

133 The sim_{acc} simulations presented here aim to model what we consider to be
 134 realistic accumulation histories of commonly used sites such as Holocene lakes
 135 or bogs. We did not invoke more chronologically disruptive features such as
 136 hiatuses, extremely variable accumulation rates, large sections without datable
 137 material or systematic ^{14}C age offsets, but this could be investigated.
 138 However, the approach we present can be applied to individual sections of
 139 sequences, as well as to whole sequences.

140 *Age-depth modelling (sim_{age})*

141 We applied four types of age-depth models, which produced thousands to
 142 millions of random iterations to provide many calendar age estimates for each
 143 core depth. We first used the popular basic model of linear interpolation as

144 implemented in *psimpoll* (Bennett, 2007) and *clam* (Blaauw, 2010), which
145 assumes that accumulation rates were constant between neighbouring dated
146 depths and changed, potentially abruptly, exactly at the dated depths
147 (Bennett, 1994). We then applied a basic model that varies more smoothly
148 over time (smooth spline in *clam*). Since ages further down a core must be
149 older, even if the dates or models suggest otherwise, software implementing
150 the above approaches can be instructed to remove any iterations with
151 age-depth model reversals after modelling. Finally, we tested two Bayesian
152 piecewise linear models that use gamma distributions as prior information in
153 order to ensure chronological ordering of each iteration. *Bchron* (Haslett and
154 Parnell, 2008) simulates steps in time and depth sampled from gamma
155 distributions, whereas *Bacon* (Blaauw and Christen, 2011) models the
156 accumulation rates of many equally spaced depth sections based on a gamma
157 distribution (here set at mean 50 and shape 1.1 to allow for many
158 accumulation rates), and a beta distribution to invoke a degree of dependence
159 in accumulation rate between neighbouring depths. Both *Bchron* and *Bacon*
160 have routines to handle outliers, whereas for basic age-depth models outliers
161 need to be removed manually. OxCal’s P_Sequence (Bronk Ramsey, 2008) was
162 also tried but individual runs and analyses interpolated to 500 1-cm intervals
163 took days instead of minutes, rendering it less suitable for these intensive
164 simulation exercises. R code (R Core Team, 2017) is available on Figshare
165 (doi:10.6084/m9.figshare.3808311).

166 All age-depth models were produced as outlined above. Each age-depth model
167 sim_{age} was then compared to the known simulated sim_{acc} age θ_d for each
168 depth d , calculating its accuracy as standardized offset, $z_d = |\bar{x}_d - \theta_d|/\sigma_d$,
169 where \bar{x}_d and σ_d are the mean and standard deviation, respectively, of the
170 modelled ages. Standardizing ensures that offsets can be compared between
171 core depths modelled at different precisions. Then the minimum, maximum
172 and mean z over all depths was taken as the age-depth model’s accuracy,
173 whereas its precision was calculated as the minimum, maximum and mean of
174 the modelled 95% confidence intervals. In this context, precision refers to the

175 degree of uncertainty in an estimate and accuracy refers to the actual error or
 176 offset of the estimate to its true value.

177 *Sequential dating (sim_{dat})*

178 After each age-depth model sim_{age} was run, we used that age-depth model to
 179 determine which depth to date next. This has been investigated by Buck and
 180 Christen (1998) and Christen and Buck (1998) using simulations that were
 181 computationally extremely time-consuming. Here we adopt a much faster
 182 sampling design score developed by Christen and Sansó (2011), which predicts
 183 which next data point among all available candidates is likely to provide the
 184 most new information. Only one candidate depth is selected at a time,
 185 although this not a realistic scenario for real-life ^{14}C dating. In future work we
 186 therefore plan to enable selecting multiple depths.

187 Let s_1, s_2, \dots, s_M be the depths at which we may take a sample to be dated
 188 (by radiocarbon or otherwise). Let d_1, d_2, \dots, d_m (a subset of the s_i) be the
 189 depths at which we already have dates $y_m = (y_1 \pm \sigma_1, y_2 \pm \sigma_2, \dots, y_m \pm \sigma_m)$.
 190 Let $cov(d_i, d_j)$ be the covariance of depths d_i and d_j calculated from the joint
 191 posterior distribution of the age-depth model using the currently dated depths,
 192 that is $G(d|y_m)$. This covariance structure may be approximated using the
 193 Monte Carlo output to estimate the chronology (Blaauw, 2010; Haslett and
 194 Parnell, 2008; Blaauw and Christen, 2011). For all iterations $t = 1, 2, \dots, T$,
 195 we calculate the covariance of the corresponding ages $G(s_i|\theta^{(t)}, x^{(t)})$ and
 196 $G(s_j|\theta^{(t)}, x^{(t)})$. Let also $V(s_i) = cov(s_i, s_i)$ be the variance at depth s_i . The
 197 score A for a new candidate depth d_{m+1} to be dated is (Christen and Sansó,
 198 2011):

$$A(d_{m+1}) = (1 - \|r(d_{m+1})\|) \frac{1}{M} \sum_{j=1}^M \frac{cov(s_j, d_{m+1})^2}{V(s_j)V(d_{m+1})},$$

199 where

$$\|r(d_{m+1})\| = \sqrt{\sum_{k=1}^m \frac{cov(d_k, d_{m+1})^2}{V(d_k)V(d_{m+1})}}.$$

200 The score has a formal justification in terms of maximizing the reduction in
 201 predictive variance of the new sample point d_{m+1} , specifically it is an
 202 approximated and computationally simple version of the sequential Active
 203 Learning Cohn strategy used in robotics (Christen and Sansó, 2011).
 204 Intuitively, the score chooses a new sample point that is correlated with other
 205 locations given the term

$$\frac{1}{M} \sum_{j=1}^M \frac{\text{cov}(s_j, d_{m+1})^2}{V(s_j)V(d_{m+1})},$$

206 and consequently favours depths with high variance in their age estimates
 207 (large uncertainties), as well as depths which inform us much about the ages of
 208 other depths in the sequence (high covariance). However, the term
 209 $1 - \|r(d_{m+1})\|$ penalizes depths correlated with locations already sampled,
 210 thus separating the dated depths (see Christen and Sansó, 2011, for further
 211 intuitive and technical justifications of the score and some examples showing
 212 its performance).

213 The same methods and results apply to the dating density of entire cores or of
 214 specific sections of cores. We note that it often makes scientific and financial
 215 sense to only apply higher dating resolutions, and thus reach higher
 216 chronological precision, for specific core sections of interest (e.g. the 1-m long
 217 sections discussed further below).

218 **RESULTS**

219 Depending on their dating density and the chosen age-depth model type,
 220 chronologies for cores from the Neotoma database reach millennial to
 221 centennial-scale precision (Figure 1). At first sight, basic age-depth models
 222 based on linear interpolation or smooth splines (Bennett, 2007; Blaauw, 2010)
 223 appear to produce more precise chronologies than do Bayesian models (Haslett
 224 and Parnell, 2008; Blaauw and Christen, 2011). At below average dating
 225 densities, adding dates enhances the precision of basic age-depth models, but
 226 this effect levels off at average and higher dating densities. This precision, even

227 with low dating densities, is due to the implicit assumption that the age-depth
228 model chosen is the true one, so the model has zero error for the choice of
229 age-depth model. Adding in error for age-depth model choice substantially
230 reduces the total precision (Bennett, 1994; Blaauw and Heegaard, 2012).
231 Bayesian age-depth models on the other hand consistently become more
232 precise as dating density increases. The same patterns appear when all but the
233 top and bottom dates are removed from the Kråkenes sequence, followed by
234 re-adding its dates one by one until reaching 20 dpm (Figure 2).
235 At the initial, lowest dating densities, most age-depth models fail,
236 unsurprisingly, to capture the long-term shapes of the simulated age-depth
237 trajectories (Telford et al., 2004; Trachsel and Telford, 2017) even though the
238 95% error ranges of the Bayesian models mostly overlap with the ‘true’ ages.
239 As a few more strategically chosen dates are added, all models improve to
240 follow a site’s main features. More complicated histories require more dates
241 (Figures 3–4, Supplementary information animations 1–4). However what
242 happens at higher dating densities depends largely on the chosen age-depth
243 model type.

244 Our simulations reveal several important implications of different approaches
245 to age-depth modelling. As with the analyses of cores from the Neotoma
246 database and Kråkenes, different model types produce very different precision
247 estimates (Figure 4a, b, e, f). The commonly used basic models of linear
248 interpolation and smooth spline appear at first sight to be pleasingly precise
249 (average 95% ranges mostly under ca 500 yr), due to the implicit zero error for
250 choice of age-depth model (see above), but the Bayesian age-depth models are
251 more realistic, reconstructing much larger uncertainties especially at low to
252 average dating densities (up to 1 dpm). However, the supposedly higher
253 precision of basic age-depth models comes at a severe cost; they are inaccurate
254 especially at low to average dating densities. Indeed, at those dating densities
255 basic age-depth models are offset from the ‘true’ ages by many standard
256 deviations; Figure 4b, d). The Bayesian models on the other hand are
257 consistently accurate and produce realistic estimates of precision, the true ages

258 lying well within two standard deviations (95%) at most depths and dating
259 densities (Figure 4f, h). Even so, in all of our simulations (basic and Bayesian)
260 and at almost all dating densities, the 95% age ranges of some depths lie
261 outside their ‘true’ ages (envelopes extending above the 2 sd limit in Figure 4).
262 Above ca 1 dpm, linear interpolation age-depth models do not become more
263 precise at increasing dating densities, whereas the smooth-spline models show
264 some improvement after reaching ca 5 dpm. However, the Bayesian models
265 keep on improving. This is because Bayesian models take advantage of
266 chronological ordering, causing ever-increasing precision (yet remaining
267 accurate) as more and more dates start to overlap. At dating densities high
268 enough to match the multi-decadal wiggles in the ^{14}C calibration curve (Kilian
269 et al., 1995; Gulliksen et al., 1998; Lohne et al., 2013; Mauquoy et al., 2002;
270 Blaauw et al., 2004; Southon et al., 2012) (Figure 5), some sections of
271 Bayesian models calculated with *Bacon* can reach multi-decadal precision.
272 Above 30 dpm even basic models gain precision again as repeated dating of
273 individual depths enhances their age estimates.

274 The curves relating dating density to model precision and, especially, accuracy
275 are not entirely smooth. Sometimes adding a few extra dates will provide an
276 extra piece of information that suddenly results in much more precise and, or,
277 accurate chronologies. However the opposite can also happen when, for
278 example, adding an extra date causes an age reversal with basic age-depth
279 models, or an outlying date produces a less accurate model (particularly for
280 linear interpolation, which is very sensitive to outliers). Bayesian models
281 calculated with *Bchron* seem to consistently lose accuracy at higher dating
282 densities (Figure 4h).

283 Our simulations show a clear impact of error size on model precision but not
284 accuracy (Figure 6). Dating scatter (Christen and Pérez E., 2009; Scott, 2013)
285 on the other hand appears to have little impact on age-depth model precision
286 (no impact for linear interpolation and a minor one for *Bacon*), but it severely
287 impacts accuracy. Model offsets increase along with increasing scatter,
288 although *Bacon*’s offsets are always considerably lower than those of linear

289 interpolation. Similarly to dating scatter, outliers have little to no impact on
290 model precision while severely affecting accuracy (Figure 6i–l). Most basic
291 age-depth models are offset by two or more standard deviations once more
292 than 20% of the dates are outlying, while *Bacon*, remarkably, remains reliable
293 until over 50% of dates are outlying.

294 **IMPLICATIONS**

295 In the early, pre-AMS, days of ^{14}C dating, dating density of cores was
296 necessarily low because slices covering many centimetres or even decimetres
297 (and thus centuries of sedimentation) had to be submitted to obtain sufficient
298 datable ^{14}C for the conventional decay counting method (e.g. Bennett et al.,
299 1992; Haberle and Lumley, 1998). With the advent of AMS dating in the 1990s
300 this limitation has largely been lifted, and prices of single dates have come
301 down in real terms. However median dating density remains below 1 dpm
302 (Figure 1), perhaps because the research community still considers 1 date per
303 millennium to be a reasonable rule-of-thumb in order to establish chronologies,
304 or because funding for chronologies has not increased (with the exception of
305 special cases where chronology is the emphasis of the study). Our simulations
306 show, however, that current typical dating densities are insufficient.
307 Commonly used basic age-depth models may fail to capture the main features
308 of a site’s accumulation history and produce highly over-optimistic precision
309 estimates (Figure 3). Increasing the dating density to ca 2 dpm, and using
310 Bayesian methods, produces age-depth models that give reasonable confidence
311 for centennial-scale precision estimates. If sub-centennial chronological
312 precision is needed (at least for selected core sections; Figure 5), dating
313 densities over 50 dpm are required, together with age-depth models that take
314 advantage of chronological ordering. Thus, chronologies should be built
315 starting with a skeleton chronology of, say, 1 date every 2 millennia (0.5 dpm),
316 after which small batches of strategically sampled depths should be dated
317 sequentially until reaching ca 2 dpm, even though this is time-consuming.

318 Basic age-depth modelling approaches such as linear interpolation remain
319 widely accepted and used within the community of past
320 climate/environmental research. For example, Shurtliff et al. (2017) argue for
321 ‘linear interpolation to be as good an approach as any’, since ‘all age-depth
322 models contain considerable uncertainty that is difficult to fully quantify’.
323 However, as a community we should ask ourselves whether these basic
324 approaches remain suited to their task (Bennett, 1994; Telford et al., 2004;
325 Trachsel and Telford, 2017). The method of linear interpolation suggests
326 higher precision in-between dated depths, and becomes more precise with
327 larger gaps between dated depths (Bennett, 1994). This unintuitive result
328 arises because this model implicitly assumes (i) that this is the true model,
329 although we know that it is not; and (ii) that ages between dated points lie
330 along a straight line, which is rarely, if ever, going to be true. Relaxing the
331 assumption (e.g., with Bayesian methods such as *Bacon*) produces the more
332 intuitive result that sections with fewer dates have higher uncertainties.
333 Bayesian models excel since they simulate many different alternative ‘routes’
334 by which a site could have accumulated in-between dated depths, diverging
335 more from the linearly-interpolated relationship if less ‘guidance’ is present.
336 Thus at low to average dating densities, Bayesian models such as *Behron* or
337 *Bacon* are preferable to basic models, since their model assumptions produce
338 more realistic reconstructions and confidence intervals. At higher dating
339 densities, the dates start to steer the models more directly and the accuracy of
340 basic and Bayesian models is comparable — though Bayesian models that
341 enforce chronological ordering can become much more precise.
342 Dating scatter seems more disruptive to age-depth model accuracy than error
343 size (Figure 6), so it makes more sense to re-date single depths (e.g. to assess
344 the reliability of dating different components) or date multiple depths
345 (constraining the ages of individually dated depths through enforcing
346 chronological ordering), rather than obtaining single high-precision dates.
347 Over past decades, the palaeoenvironmental community has repeatedly been
348 warned to take uncertainties into account (Maher, 1972; Bennett, 1994;

349 Blaauw et al., 2007; Blaauw, 2010; Jackson, 2012). Dating uncertainties
350 should not be abused by uncritically linking events between sites (Blaauw,
351 2012), nor camouflaged by plotting fossil-based reconstructions against
352 calendar time as single curves without any error visualisation. Basic age-depth
353 models, especially those based on the hugely popular linear interpolation, are
354 highly sensitive to outliers and severely overestimate precision at low to
355 average dating densities. Moreover, because they do not improve beyond ca
356 1–2 dpm, they under-perform at above-average dating densities. In contrast,
357 Bayesian approaches provide the most accurate age-depth models, with
358 reliable precision estimates throughout an impressive range of dating density
359 and quality, continually improving as dating density improves. We strongly
360 recommend aiming for dating densities ≥ 2 dpm (e.g. 20 or more dates along a
361 Holocene sequence) with realistic and stated error estimates. If this is not
362 realistically achievable for an entire sequence, it should be achieved for any
363 shorter sections where the most precise chronology is needed to meet the
364 objectives of the investigation. This will require a modest increase in funds for
365 dating and higher usage of available Bayesian age-depth models, but will
366 provide the accuracy and precision needed to interpret and correlate
367 chronologies at the level required for most palaeoenvironmental questions.

368 **ACKNOWLEDGEMENTS**

369 This work was partly funded by a Banco Santander travel grant to MB.
370 Thanks to Andrew Parnell for help with *Bchron* and to Simon Goring for
371 releasing R code to extract sites from the Neotoma Paleoecology database
372 (<http://www.neotomadb.org>); the work of the data contributors and the
373 Neotoma community is gratefully acknowledged. We are also grateful to the
374 Past Earth Network (<http://www.pastearth.net/>) for writing support (grant
375 number EP/M008363/1).

376 **References**

- 377 Bennett, K. D., 1994. Confidence intervals for age estimates and deposition
378 times in late-Quaternary sediment sequences. *The Holocene* 4, 337–348.
- 379 Bennett, K. D., 2007. *psimpoll* and *pscomb* programs for plotting and analysis.
380 URL <http://www.chrono.qub.ac.uk/psimpoll/psimpoll.html>
- 381 Bennett, K. D., Boreham, S., Sharp, M. J., Switsur, V. R., 1992. Holocene
382 history of environment, vegetation and human settlement on Catta Ness,
383 Lunnasting, Shetland. *Journal of Ecology* 80, 241–273.
- 384 Bennett, K. D., Fuller, J. L., 2002. Determining the age of the mid-Holocene
385 *Tsuga canadensis* (hemlock) decline, eastern North America. *The Holocene*
386 12, 421–429.
- 387 Blaauw, M., 2010. Methods and code for classical age-modelling of
388 radiocarbon sequences. *Quaternary Geochronology* 5, 512–518.
- 389 Blaauw, M., 2012. Out of tune: the dangers of aligning proxy archives.
390 *Quaternary Science Reviews* 36, 38–48.
- 391 Blaauw, M., Christen, J. A., 2011. Flexible paleoclimate age–depth models
392 using an autoregressive gamma process. *Bayesian Analysis* 3, 457–474.
- 393 Blaauw, M., Christen, J. A., Mauquoy, D., van der Plicht, J., Bennett, K. D.,
394 2007. Testing the timing of radiocarbon-dated events between proxy
395 archives. *The Holocene* 17, 283–288.
- 396 Blaauw, M., Heegaard, E., 2012. Estimation of age–depth relationships. In:
397 Birks, H. J. B., Juggins, S., Lotter, A., Smol, J. P. (Eds.), *Tracking*
398 *Environmental Change Using Lake Sediments, Developments in*
399 *Paleoenvironmental Research* 5. Springer, Dordrecht, pp. 379–413.
- 400 Blaauw, M., van Geel, B., van der Plicht, J., 2004. Solar forcing of climatic
401 change during the mid-Holocene: indications from raised bogs in The
402 Netherlands. *The Holocene* 14, 35–44.

- 403 Bronk Ramsey, C., 2008. Deposition models for chronological records.
404 Quaternary Science Reviews 27, 42–60.
- 405 Bronk Ramsey, C., Higham, T., Leach, P., 2004. Towards high-precision AMS:
406 Progress and limitations. Radiocarbon 46, 17–24.
- 407 Buck, C. E., Christen, J. A., 1998. A novel approach to selecting samples for
408 radiocarbon dating. Journal of Archaeological Science 25, 303–310.
- 409 Christen, J. A., Buck, C. E., 1998. Sample selection in radiocarbon dating.
410 Applied Statistics 47, 543–557.
- 411 Christen, J. A., Pérez E., S., 2009. A new robust statistical model for
412 radiocarbon data. Radiocarbon 51, 1047–1059.
- 413 Christen, J. A., Sansó, B., 2011. Advances in the sequential design of
414 computer experiments based on active learning. Communications in
415 Statistics — Theory and Methods, 4467–4483.
- 416 Goring, S., Dawson, A., Simpson, G. L., Ram, K., Graham, R. W., Grimm,
417 E. C., Williams, J. W., 2015. neotoma: A programmatic interface to the
418 Neotoma Paleocological Database. Open Quaternary 1 (2).
- 419 Groot, M. H. M., van der Plicht, J., Hooghiemstra, H., Lourens, L. J., Rowe,
420 H. D., 2014. Age modelling for Pleistocene lake sediments: A comparison
421 of methods from the Andean Fúquene Basin (Colombia) case study.
422 Quaternary Geochronology 22, 144–154.
- 423 Gulliksen, S., Birks, H. H., Possnert, G., Mangerud, J., 1998. A calendar age
424 estimate of the Younger Dryas–Holocene boundary at Kråkenes, western
425 Norway. The Holocene 8, 249–259.
- 426 Haberle, S. G., Lumley, S. H., 1998. Age and origin of tephra recorded in
427 postglacial lake sediments to the west of the southern Andes, 44°S to 47°S.
428 Journal of Volcanology and Geothermal Research 84, 239–256.

- 429 Haslett, J., Parnell, A. C., 2008. A simple monotone process with application
430 to radiocarbon-dated depth chronologies. *Journal of the Royal Statistical*
431 *Society, Series C* 57, 399–418.
- 432 Jackson, S. T., 2012. Representation of flora and vegetation in Quaternary
433 fossil assemblages: known and unknown knowns and unknowns. *Quaternary*
434 *Science Reviews* 49, 1–15.
- 435 Kilian, M. R., van der Plicht, J., van Geel, B., 1995. Dating raised bogs: new
436 aspects of AMS ^{14}C wiggle matching, a reservoir effect and climatic change.
437 *Quaternary Science Reviews* 14, 959–966.
- 438 Lohne, Ø. S., Mangerud, J., Birks, H. H., 2013. Precise ^{14}C ages of the Vedde
439 and Saksunarvatn ashes and the Younger Dryas boundaries from western
440 Norway and their comparison with the Greenland Ice Core (GICC05)
441 chronology. *Journal of Quaternary Science* 28, 490–500.
- 442 Maher, Jr, L. J., 1972. Absolute pollen diagram of Redrock Lake, Boulder
443 County, Colorado. *Quaternary Research* 2, 531–553.
- 444 Mauquoy, D., van Geel, B., Blaauw, M., van der Plicht, J., 2002. Evidence
445 from northwest European bogs shows ‘Little Ice Age’ climatic changes
446 driven by variations in solar activity. *The Holocene* 12, 1–6.
- 447 Parnell, A. C., Buck, C. E., Doan, T. K., 2011. A review of statistical
448 chronology models for high-resolution, proxy-based holocene
449 palaeoenvironmental reconstruction. *Quaternary Science Reviews* 30,
450 2948–2960.
- 451 R Core Team, 2017. R: A language and environment for statistical computing.
452 R Foundation for Statistical Computing. Vienna, Austria.
453 URL <https://www.R-project.org>
- 454 Reimer, P. J., Bard, E., Bayliss, A., Beck, J. W., Blackwell, P. G., Ramsey,
455 C. B., Buck, C. E., Cheng, H., Edwards, R. L., Friedrich, M., Grootes,

456 P. M., Guilderson, T. P., Hafidason, H., Hajdas, I., Hatté, C., Heaton,
457 T. J., Hoffmann, D. L., Hogg, A. G., Hughen, K. A., Kaiser, K. F., Kromer,
458 B., Manning, S. W., Niu, M., Reimer, R. W., Richards, D. A., Scott, E. M.,
459 Southon, J. R., Staff, R. A., Turney, C. S. M., van der Plicht, J., 2013.
460 IntCal13 and Marine13 radiocarbon age calibration curves 0-50,000 years cal
461 BP. *Radiocarbon* 55, 1869–1887.

462 Scott, E. M., 2013. Radiocarbon dating — sources of error. In: Mock, C. J.,
463 Elias, S. A. (Eds.), *Encyclopedia of Quaternary Science*. Elsevier,
464 Amsterdam, pp. 324–328.

465 Shurtliff, R. A., Nelson, S. T., McBride, J. H., Rey, K. A., Tucker, J. C.,
466 Godwin, S. B., Tingey, D. G., 2017. A 13 000 year multi-proxy climate
467 record from central Utah (western USA), emphasizing conditions leading to
468 large mass movements. *Boreas* 46, 308–324.

469 Southon, J., Noronha, A. L., Cheng, H., Edwards, R. L., Wang, Y., 2012. A
470 high-resolution record of atmospheric ^{14}C based on Hulu Cave speleothem
471 H82. *Quaternary Science Reviews* 33, 32–41.

472 Telford, R. J., Heegaard, E., Birks, H. J. B., 2004. All age–depth models are
473 wrong: but how badly? *Quaternary Science Reviews* 23, 1–5.

474 Trachsel, M., Telford, R. J., 2017. All agedepth models are wrong, but are
475 getting better. *The Holocene* 27, 860–869.

476 **Figure captions**

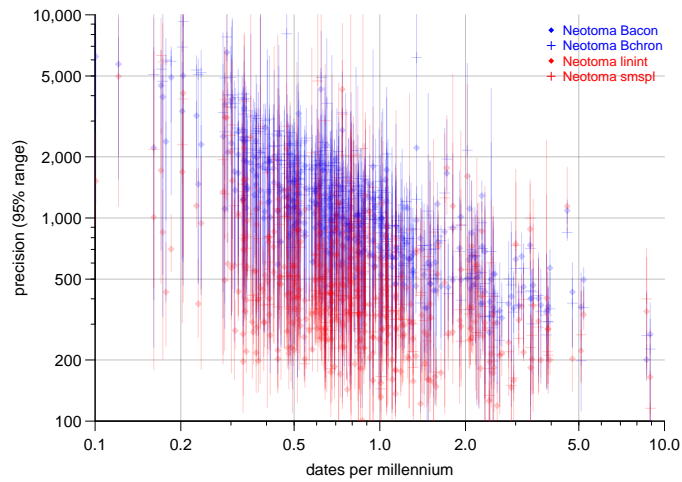


Figure 1: Dating density (dates per millennium) and age-depth model precision (95% error ranges) of all 356 ^{14}C -dated cores spanning at least 500 yr and having at least 2 ^{14}C dates, extracted from the Neotoma Database using R code (Goring et al., 2015). Vertical lines and symbols indicate the minimum to maximum mean age-depth model precision of each core. Red shows basic age-depth models (diamonds linear interpolation, crosses smooth spline), blue Bayesian (diamonds *Bacon*, crosses *Bchron*). Note logarithmic axes.

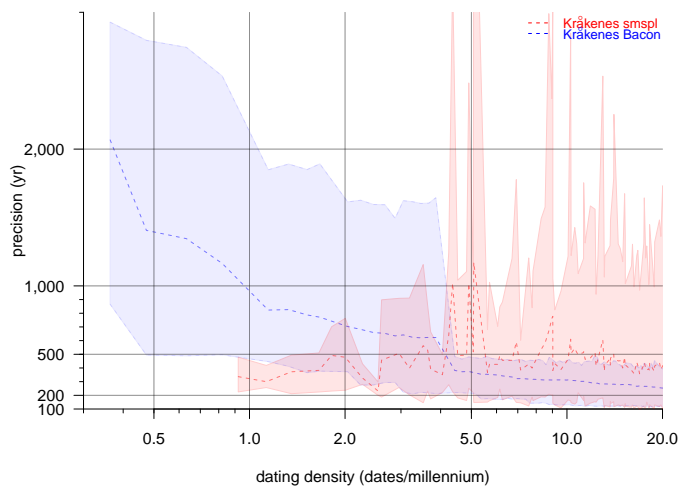


Figure 2: Dating density (dates per millennium) and age-depth model precision (95% error ranges) of the high-resolution dated Kråkenes record (Gulliksen et al., 1998; Lohne et al., 2013). Shaded envelopes and dashed curves show minimum to maximum resp mean age-depth model precision upon sequential re-sampling of the record (red smooth spline (smspl), blue *Bacon*). Note logarithmic axes.

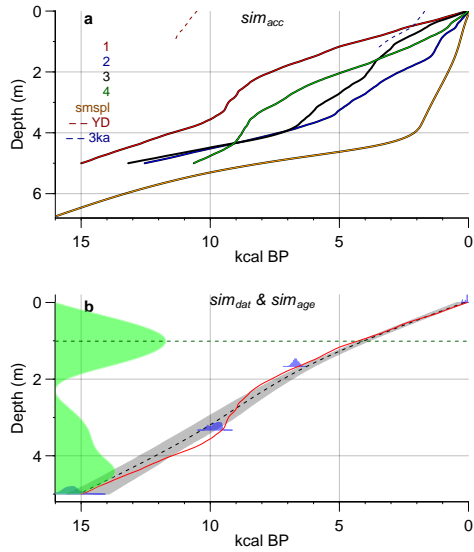


Figure 3: The three-stage simulation of sedimentation, sequential dating, and age-depth modelling. The upper panel shows seven *sim_{acc}* simulations using a range of random seeds (1: 5113, 2: 2995, 3: 5993, 4: 6993), a smooth spline (smspl) through the “Example” core provided with *clam* (Blaauw, 2010) (orange), simulation 11136 (Younger Dryas) and simulation 1102 (at 3 kcal BP Hallstatt Plateau). The lower panel shows the sequential process of selecting which depth to date next, producing the resulting age-depth model, and comparing the model to the known ages. In this example, so far four depths have been dated (blue silhouettes; *sim_{dat}*) from the simulated core (red curve; *sim_{acc}*). A smooth-spline age-depth model is drawn through these dates (grey envelope and dashed black line; *sim_{age}*). Its age estimates can be compared to the ‘true’ history (red). From the sample spacing and the age-depth model’s variance and covariance at each depth a sampling score is calculated (green distribution). The depth of 1 m has the highest score (dashed green line) and will thus be dated next.

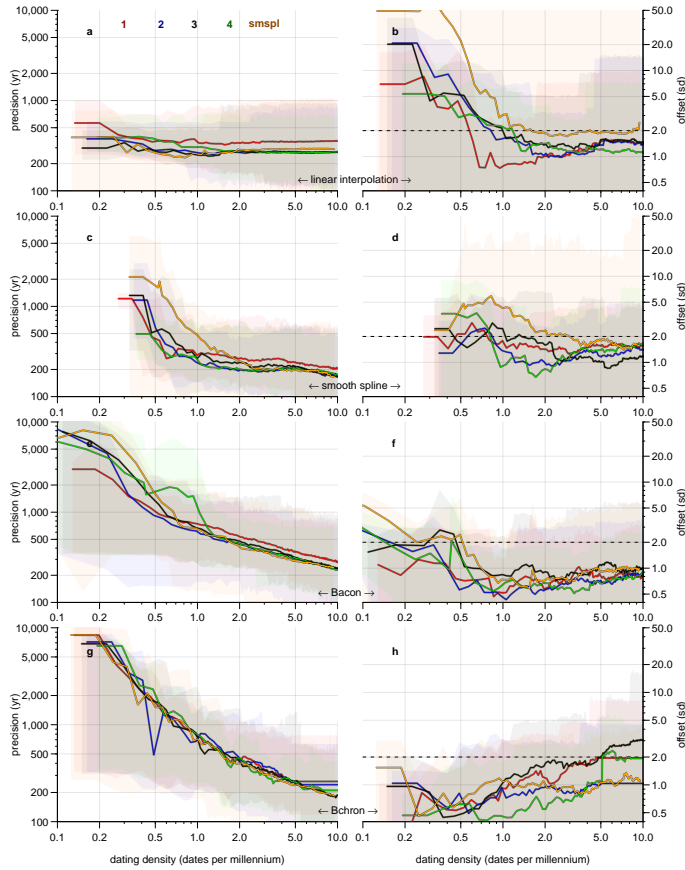


Figure 4: Impact of dating density on chronological precision and accuracy using basic (a-b, linear interpolation; c-d, smooth spline) and Bayesian (e-f, *Bacon* (Blaauw and Christen, 2011); g-h, *Bchron* (Haslett and Parnell, 2008)) age-depth models. For each of 5 simulated cores (see Figure 3 for key to colours), sim_{acc} , dates were added sequentially (sim_{dat} , up to 150 dates) and age-depth models constructed (sim_{age}). Curves show mean values and envelopes show minimum to maximum values for age-depth model precision (95% error ranges, left panels) and accuracy (standardized offset from ‘true’ ages, right panels; dashed curve shows 2 standard deviation offset). Note logarithmic axes.

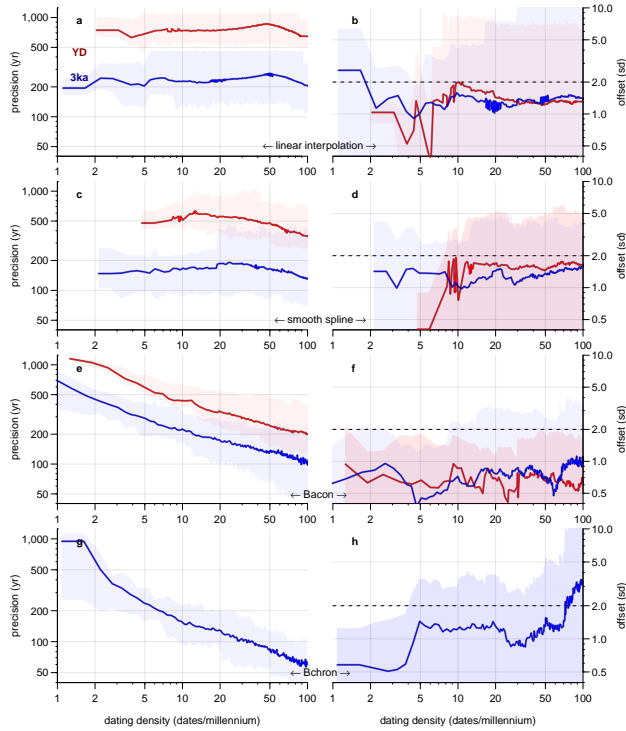


Figure 5: Impact on model reliability of high dating densities at periods with major wiggles in the IntCal13 ^{14}C calibration curve (Reimer et al., 2013) for a range of age-depth model types (a-b linear interpolation, c-d smooth spline, e-f *Bacon*, g-h *Bchron*). Red curves indicates simulation 11136 (see Figure 2) focusing on the Younger Dryas Period; blue curves shows simulation 1102 around the 3 kcal BP Hallstatt Plateau. Precision and accuracy are shown in left and right panels, respectively. At high dating densities, single depths are dated several times, causing conflicting age estimates and resulting in unsuccessful *Bchron* runs for the YD simulation. Note logarithmic axes.

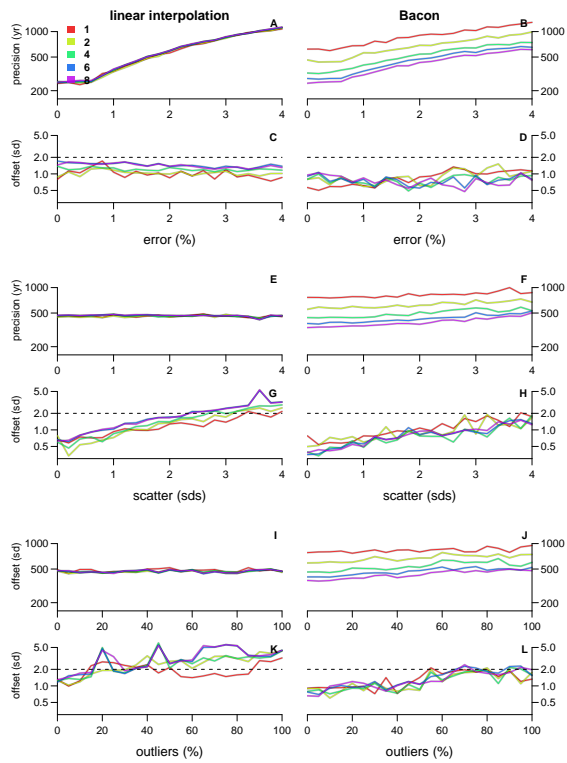


Figure 6: Impact of laboratory error (a-d), dating scatter (e-h) and outliers (i-l) on model reliability. Left panels show linear interpolation, right panels *Bacon*. Curves show mean precision and accuracy at a range of dpm (see legend in panel a). Given the time-consuming nature of these simulations, results are available only for linear interpolation and *Bacon*.